AD-A143 769 THE GAS PHASE STRUCTURE OF AZIDOTRIFLUOROMETHANE AN ELECTRON DIFFRACTION..(U) ROCKWELL INTERNATIONAL CANOGA PARK CA ROCKETDYNE DIV K O CHRISTE ET AL. 23 JUL 84 1/1

UNCLASSIFIED RI/RD84-183 N00014-83-C-0531 F/G 7/4 NL

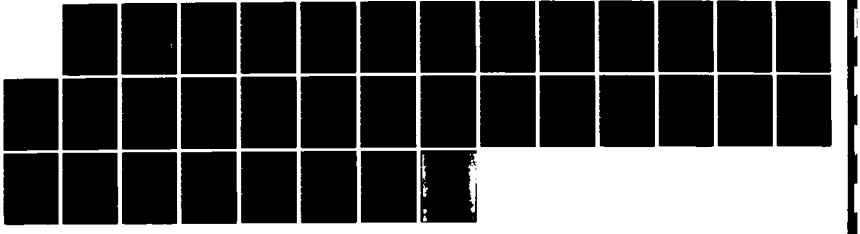

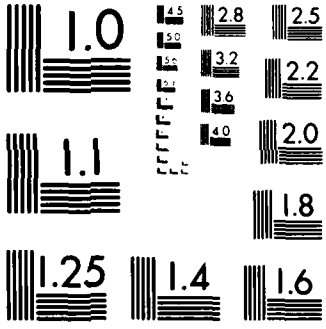

(12)

Unclassified

SECURITY CLASSIFICATION OF THIS PAGE (When Data Entered)

REPORT DOCUMENTATION PAGE	READ INSTRUCTIONS BEFORE COMPLETING FORM
1. REPORT NUMBER: Technical Report 1	2. GOVT ACCESSION NO.: AD-A143 769
	3. RECIPIENT'S CATALOG NUMBER
4. TITLE (and Subtitle): The Gas Phase Structure of Azidotrifluoromethane. An Electron Diffraction, Microwave Spectroscopy and Normal Coordinate Analysis.	5. TYPE OF REPORT & PERIOD COVERED: Technical Report
	6. PERFORMING ORG. REPORT NUMBER: RI/RD84-183
7. AUTHOR(s): Karl O. Christe, Dines Christen, Heinz Oberhammer and Carl J. Schack	8. CONTRACT OR GRANT NUMBER(s): N00014-83-C-0531
9. PERFORMING ORGANIZATION NAME AND ADDRESS: Rocketdyne, 6633 Canoga Avenue, Canoga Park, CA 91304; University of Tubingen, Tubingen 7400 Tubingen, West Germany	10. PROGRAM ELEMENT, PROJECT, TASK AREA & WORK UNIT NUMBERS: NR 053-840
11. CONTROLLING OFFICE NAME AND ADDRESS: Office of Naval Research, Department of the Navy, Arlington, Virginia 22217	12. REPORT DATE: July 23, 1984
	13. NUMBER OF PAGES: 28
14. MONITORING AGENCY NAME & ADDRESS (if different from Controlling Office)	15. SECURITY CLASS (of this report): Unclassified
	15a. DECLASSIFICATION/DOWNGRADING SCHEDULE

16. DISTRIBUTION STATEMENT (of this Report)

Approved for public release; distribution unlimited

17. DISTRIBUTION STATEMENT (of the abstract entered in Block 20, if different from Report)

DTIC ELECTE JUL 26 1984 S D B

18. SUPPLEMENTARY NOTES

To be published in Inorganic Chemistry

19. KEY WORDS (Continue on reverse side if necessary and identify by block number)

Azidotrifluoromethane
gas phase structure
Microwave
Electron diffraction
Normal coordinate anlaysis

20. ABSTRACT (Continue on reverse side if necessary and identify by block number)

The geometric structure of azidotrifluoromethane has been obtained by a combined analysis of electron diffraction intensities and ground state rotational constants derived from the microwave spectrum.

84 07 26 018

Continued (Page 2)

DD FORM 1 JAN 73 1473 EDITION OF 1 NOV 65 IS OBSOLETE

Unclassified

SECURITY CLASSIFICATION OF THIS PAGE (When Data Entered)

The following parameters were obtained (r_{av}-values in Å and deg. with 2σ uncertainties in units of the last decimal): C-F = 1.328(2), $C-N_\alpha$ = 1.425(5), $N_\alpha-N_\beta$ = 1.252(5), $N_\beta-N_\omega$ = 1.118(3), $\angle CN_\alpha N_\beta$ = 112.4(2), $\angle N_\alpha N_\beta N_\omega$ = 169.6(34) and ∠FCF = 108.7(2). The CF_3 group is in the staggered position with respect to the N_3 group and tilted away from it by 5.8(4)°.

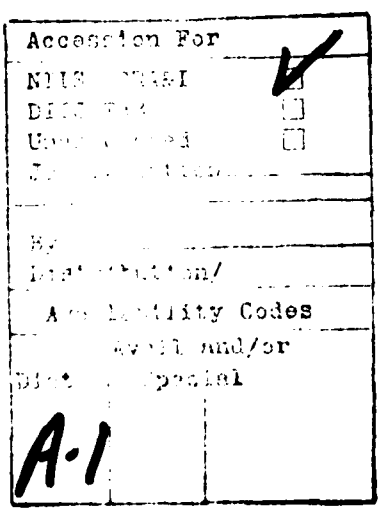

OFFICE OF NAVAL RESEARCH

Contract N00014-83-C-0531

Task No. NR 053-840

TECHNICAL REPORT NO. 1

The Gas Phase Structure of Azidotrifluoromethane. An Electron Diffraction, Microwave Spectroscopy and Normal Coordinate Analysis.

by

Karl O. Christe, Dines Christen, Heinz Oberhammer, and Carl J. Schack

Rocketdyne
A Division of Rockwell International
Canoga Park, CA 91304

University of Tübingen
Institut fur Physikalische und
Theoretische Chemie
7400 Tübingen
W Germany

July 23, 1984

Prepared for publication in Inorganic Chemistry

Contribution from the Institut für Physikalische und Theoretische Chemie der Universität Tübingen, 7400 Tübingen, West Germany, and Rocketdyne, A Division of Rockwell International Corporation, Canoga Park, California 91304

THE GAS PHASE STRUCTURE OF AZIDOTRIFLUOROMETHANE. AN ELECTRON DIFFRACTION, MICROWAVE SPECTROSCOPY AND NORMAL COORDINATE ANALYSIS

Karl O. Christe,[1a] Dines Christen,[1b] Heinz Oberhammer,*[1b] and Carl J. Schack[1a]

ABSTRACT

The geometric structure of azidotrifluoromethane has been obtained by a combined analysis of electron diffraction intensities and ground state rotational constants derived from the microwave spectrum.

The following parameters were obtained (r_{av}-values in Å and deg. with 2σ uncertainties in units of the last decimal): C-F = 1.328(2), $C-N_\alpha$ = 1.425(5), $N_\alpha-N_\beta$ = 1.252(5), $N_\beta-N_\omega$ = 1.118(3), $\sphericalangle CN_\alpha N_\beta$ = 112.4(2), $\sphericalangle N_\alpha N_\beta N_\omega$ = 169.6(34) and $\sphericalangle FCF$ = 108.7(2). The CF_3 group is in the staggered position with respect to the N_3 group and tilted away from it by 5.8(4)°.

INTRODUCTION

Structural data on covalent azides are rare due to the explosive nature[2,3] and handling difficulties encountered with these compounds. One of the more stable covalent azides is CF_3N_3, a

compound originally prepared by Makarov and coworkers[4,5] and recently studied in more detail by two of us[6]. Although the closely related CH_3N_3 molecule has previously been studied by both electron diffraction[7] and microwave spectroscopy[8], the available data were insufficient to determine whether the N_3 group is linear, and to obtain a reliable value for the tilt angle of the methyl group. Furthermore, a comparison of the structures of CH_3N_3 and CF_3N_3 was expected to contribute to our knowledge of how the substitution of a CH_3 group by a CF_3 group influences the structure of the rest of the molecule[9].

EXPERIMENTAL SECTION

Synthesis and Handling of CF_3N_3. The sample of CF_3N_3 was prepared as previously described[6]. Prior to the electron diffraction experiments, a small amount of N_2 formed by decomposition of some CF_3N_3 was pumped off at -196°C. The only other decomposition products were nonvolatile and therefore did not interfere with the measurements.

Electron Diffraction. The scattering intensities were recorded with the Balzers gas diffractograph at two camera distances (25 and 50 cm) on Kodak electron image plates (13 x 18 cm). The accelerating voltage was about 60 kV. The sample was cooled to -80°C and the nozzle temperature was 15°C. The camera pressure never exceeded 2.10^{-5} torr during the experiment. Exposure time was 6-9 sec for the long, and 15-25 sec for the short camera distance. The electron wavelength was calibrated with ZnO diffraction patterns. Two plates for each camera distance were analyzed by the usual procedures. Background scattering recorded without gas was subtracted from the 25 cm data. Averaged molecular intensities for both camera distances

($s = 1.4 - 17$ and $8 - 35 \text{Å}^{-1}$) are presented in Fig. 1 and numerical values for the total scattering intensities are available as supplementary data[10].

Microwave Spectroscopy. The microwave spectrum was recorded at temperatures between -70° and -40°C at pressures around 10 mtorr, and at frequencies between 7 and 25 GHz (X- and K-Band) using a standard 100 kHz Stark spectrometer.

CF_3N_3 was initially flowed through the cell, but since the sample proved to be very stable, it was only changed at hours' intervals.

An initial broad band sweep in K-band, applying a 0-20 V ramp voltage at the external sweep connector of the Marconi sweeper, immediately revealed the μ_a R-branch heads typical of a near prolate rotor, and thus restricted the ranges to be searched.

STRUCTURE ANALYSIS

A preliminary analysis of the radial distribution function (Fig. 2) clearly demonstrates that the CF_3 group is staggered with respect to the N_3 chain. Model calculations for the eclipsed configuration result in very bad agreement with the experimental data in the range $r > 2.5$ Å (see Fig. 2). The radial distribution function for the eclipsed configuration was calculated with the final geometric parameters derived for the staggered conformation. Increase of the $CN_\alpha N_\beta$ angle to about 130° improved the fit for the peak at 3.3 Å but the disagreement for the peaks around 2.7 and 4.5 Å remained. Therefore, in the following analysis the CF_3 group was constrained to the staggered position. However, small torsional deviations (<10°) from this position cannot definitely be excluded.

In the least squares analysis a diagonal weight matrix was applied to the intensities and scattering amplitudes, and the phases of J. Haase[11] were used. The spectroscopic corrections, Δr (Table 1), were incorporated in the refinement. For torsional vibrations, the concept of perpendicular (rectilinear) amplitudes results in unrealistically large contributions to these corrections for torsion independent distances (C-F, F..F and N..F). Therefore, contributions from the CF_3 torsion, which is a large amplitude vibration, were neglected for torsion independent distances[12]. Assuming local C_{3v} symmetry for the CF_3 group with a possible tilt angle between the C_3 axis and the C-N bond, eight geometric parameters (including the $N_\alpha N_\beta N_\omega$ angle) are required for the determination of the structure of CF_3N_3. These parameters were refined simultaneously with six vibrational amplitudes (see Table 1). The remaining vibrational amplitudes which either cause high correlations or are badly determined in the electron diffraction experiment, were constrained to the spectroscopic values, calculated from the force field. This is justified, since the refined amplitudes agree very well with the spectroscopic values. The result from the electron diffraction analysis is included in Tables 1 and 2.

In the final stage of the analysis, structural parameters were fitted to electron diffraction intensities as well as rotational constants[13]. Although the method for calculating $\Delta B^i = B_o^i - B_z^i$ is based on the assumption of small amplitude vibrations, which certainly does not describe the torsional motion, this approximation has a minor effect on the determination of the geometric parameters. In order to test this effect, structural parameters were calculated using three different corrections: (1) assuming all vibrations to have small amplitudes (ΔA = 0.39, ΔB = 1.98 and ΔC = -0.78 MHz), (2) disregarding torsion (ΔA = 4.42, ΔB = 1.16 and ΔC = 1.22 MHz) and (3) no corrections at all. The relative weight between electron diffraction and microwave data was adjusted, until the rotational constants were fitted to within 20% of the corrections in case (1) and (2) and to within 1 MHz in case (3). These calculations demonstrate that the small differences in the rotational constants do not affect the geometric parameters outside the error limits given in Table 2.

The results demonstrate the usefulness of the rotational constants for the reduction of the uncertainties in the $CN_\alpha N_\beta$- and the CF_3 tilt angle, which are very sensitive to the asymmetry or, in other words, to B_z-C_z.

NORMAL COORDINATE ANALYSIS

A force field, required for the joint analysis of microwave and electron diffraction data, was derived from the 14 fundamental frequencies determined in a previous study[6], the torsional frequency, derived from relative intensity measurements of rotational transitions of the excited torsional states, and the centrifugal distortion constant D_{JK}, determined from the rotational spectrum of the ground state.

Valence force constants were refined with the program NCA[14] based on mass weighted cartesian coordinates. The modified harmonic force field (Table 3) looks reasonable, but is, of course, underdetermined.

The mean deviation between measured and calculated frequencies is $\overline{\Delta\nu} = 4\ cm^{-1}$.

ROTATIONAL SPECTRUM

The assignment of the band heads in the K-band region to the J: 4→5 (19.62 GHz) and J: 5→6 (23.54 GHz) transitions was straightforward since these band heads appeared very close to the frequencies predicted by the preliminary electron diffraction model (B+C = 3.94 GHz), but the high resolution recordings did not openly display the characteristic pattern of a near prolate (K = -0.989) rotor (see

Fig. 3). The deviations arise from excited vibrational states - especially the low lying torsional states - as will be discussed below. The frequencies of all measured transitions and the ensuing rotational constants have been collected in Table 4. The $K_{-1} = 1$ lines stand out quite clearly, though, and recording at different Stark fields permitted the identification of $K_{-1} = 0$ lines which appear only at high fields. Subsequently higher K_{-1}-lines were identified, but because many of them are subject to heavy overlapping, some of them could only be measured using a radio frequency/microwave double resonance technique (RFMWDR) as described below.

The lowest J-lines show signs of quadrupole hyperfine structure, but no attempt was made to resolve and analyze these splittings. Stark measurements on different M-components of the transitions $4_{14} \rightarrow 5_{15}$, $4_{13} \rightarrow 5_{14}$, $\rightarrow 5_{15} \rightarrow 6_{16}$ and $5_{14} \rightarrow 6_{15}$ (calibrating the field against the OCS shifts and using Muenter's value for its dipole moment[15]) yielded a dipole moment in the a-direction of $\mu_a = 1.15(10)$ D.

To understand the microwave spectrum in detail, especially the many lines between the two $K_{-1} = 1$ transitions, it is necessary to consider the possible molecular vibrations. In an earlier study[6], the vibrational spectra were investigated and 14 of the 15 fundamentals identified. The missing one, the torsion of the CF_3 group, was predicted to lie below 90 cm^{-1}, but could not experimentally be observed.

Fig. 4 shows the $5_{15} \rightarrow 6_{16}$ transition in a highly amplified recording. From the characteristic Stark patterns it is possible to identify all of the obvious lines with the same transition, only in different vibrational states. The very intense progression to higher frequency must be assigned to the torsion, and relative intensity

measurements using the Wilson-Nesbitt method[16] yield an energy above the ground state of 47(3) cm^{-1} for the first excited torsional state and thus for the torsional frequency.

To test the reliability of this method, the energy of excited states of other vibrations were determined and compared to the fundamental frequency determined from the IR and Raman spectra (in parenthesis): ν_{10}: 177 (179), ν_9: 409 (402). ν_{14}: 459 (450), $\nu_{10}+\nu_{15}$: 221 cm^{-1} comprised of ν_{10}: 174 and ν_{15}: 47 cm^{-1}.

The reliability of the method obviously decreases with increasing frequency (decreasing intensity) and the method fails for transitions falling between the two $K_{-1} = 1$ lines because of serious overlapping of lines and Stark components.

Examination of the $5_{14} \rightarrow 6_{15}$ transitions to determine their relative intensities revealed that the ν_{15} progression extends toward lower frequencies, and thus the frequency difference between the $K_{-1} = 1$ lines decreases with increasing excitation of ν_{15}. This effect is not observed with the other excited states (notably ν_{10}). The frequency difference between the $K_{-1} = 1$ lines directly determines B-C, and thus the observed trend indicates an increase in symmetry in the ν_{15} progression.

In order to explain this trend, it must be noted that a structural model having the C_3 axis of the CF_3 group colinear with the C-N bond, only produces a B-C value of 1-2 MHz. To reproduce the observed B-C value for the ground state (20.5 MHz) it is necessary to assume a tilt angle of $\sim 5°$.

Consequently, one could propose that the effect of higher torsional excitation is the removal of the tilt of the CF_3 group. In that case one would expect higher torsional states to have B-C values between 1 and 2 MHz.

On the other hand, if one realizes that most of the molecular mass is concentrated in the trifluoro methyl group, it is possible to visualize the light "frame" rotating about the heavy "top" and higher excitation would lead to an effective symmetric top molecule with the excited energy levels lying well above the barrier to the torsional motion. In that case, however, as the energy levels approach the top of the barrier, tunnelling through the threefold barrier would cause the rotational lines to split into nondegenerate A and doubly degenerate E components.

Unfortunately, this splitting is expected to take place at the frequency where the center of the rotational transitions of the excited torsional states have "turned back" (see Fig. 3) into the upper $K_{-1} = 1$ lines of the lower torsional states, and thus it is impossible to clearly distinguish the weaker lines of the higher excited states.

It was hoped that double resonance experiments (RFMWDR) could circumvent this problem[17] RFMWDR techniques were used to identify and measure the J: 5→6, $K_{-1} = 2$ transitions of the molecule in its ground as well as first excited torsional state, using a pump frequency of 3.1 MHz, which happens to be the asymmetry splitting of the J=5 levels for the ground state and the splitting of the J=6 levels of the first excited torsional state. Using a pump frequency of 6.15 MHz (the ground state splitting of the J=6 levels) only the ground state transitions are observed.

It was also possible to observe the $K_{-1} = 1$ lines in RFMWDR (J: 5→6) for the ground (ν_p = 307.0 MHz), the 1st excited torsional (ν_p = 218.4 MHz), the 2nd (ν_p = 128.7 MHz) and barely the 3rd excited torsional state (ν_p = 36.1 MHz).

The weakness of the 3rd excited torsional state transitions extinguished the hope of finding the $v_{15} = 4$ lines using the DR-technique, which would otherwise have overcome the problem of overlapping.

Fortunately, however, the J: 1→2 transitions around 7.9 GHz (Fig. 5), modulated at a Stark field of 800 V/cm only show the $K_{-1} = 0$ transitions, and thus provide a somewhat clearer picture. It looks like the $v_{15} = 3$ transition is somewhat broadened compared to the $v_{15} = 0$, 1 and 2 transitions, and the $v_{15} = 4$ transition is possibly split into two components, indicating a torsional level approaching the top of the barrier.

The assumption of a purely sinusoidal potential allows a determination of the barrier heights from the torsional force constant, known from the normal coordinate analysis

$$\text{f.c.} = \frac{\partial^2 V}{\partial \alpha^2} = \frac{\partial^2}{\partial \alpha^2}\left(\frac{V_3}{2}(1 - \cos 3\alpha)\right) \text{ at } \alpha = 0 = \frac{9V_3}{2}$$

or: 0.03 mdyn Å^2 = 4.35 kcal/mol = $\frac{9V_3}{2}$; V_3 = 0.97 kcal/mol.

Thus, the $v_{15} = 4$ state with an energy of .675 kcal is in fact quite close to the top of the barrier, especially since the addition of a few per cent V_6 potential would somewhat lower the value of V_3. It seems, although the evidence is sparse, that the decrease in B-C on excitation of v_{15} is due to the hindered internal rotation of the trifluoro methyl group.

DISCUSSION

The most significant features of the CF_3N_3 structure are the bond lengths, the nonlinearity of the N_3 group, and the torsion and tilt angle of the CF_3 group with respect to the N_3 group. These features are discussed in the following paragraphs.

Bond Lengths. The above results clearly demonstrate that in CF_3N_3 the N_β-N_ω bond is significantly shorter than the N_β-N_α bond. This can be attributed to the electron withdrawing effect of the CF_3 group. A comparison of the MN_3 series (M = alkali metal, $(CH_3)_3Si$, H, Cl, CF_3) shows that if M is of very low electronegativity, as for example in the alkali metals, we have an ionic $M^+N^-_3$ structure (I) with two degenerate N-N bonds of 1.16Å each. With increasing electronegativity of M, the M-N bond becomes more covalent and the contribution from the resonance structure (III) increases, due to the electron withdrawing effect of M. This causes an increase in the bond length difference between N_β-N_ω and N_β-N_α (see Table 5).

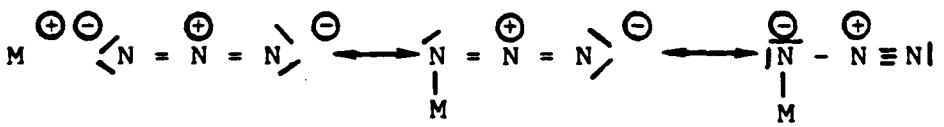

(I) (II) (III)

A comparison of the C-N bond lengths in CH_3N_3 and CF_3N_3 also shows the expected effect[9]. Replacement of the CH_3 by the CF_3 group results in bond shortening if the groups are bonded to electronegative atoms or groups. Hence the C-N bond in CF_3N_3 (1.425Å) is significantly shorter than that in CH_3N_3 (1.468Å).

Torsional Angle of the CX_3 Group. In general methyl or trifluoro methyl groups prefer the staggered position with respect to single bonds, but prefer an eclipsed position with respect to double bonds. Representative examples in the case of C=C double bonds are: $CX_3CH=CH_2$[22] and trans $CX_3CH=CHCX_3$[23,24]. Only strong steric repulsions can force CF_3 groups to abandon the eclipsed position, such as in cis $CF_3CH=CHCF_3$[24]. Only one example is known for N=N double bonds: trans $CX_3N=NCX_3$[24,25,26], where the CX_3 groups again eclipse the N=N double bond and stagger the N lone pair. In CF_3N_3 the CF_3 group occupies a staggered position with respect to the N_3 group as shown by (IV), and this indicates

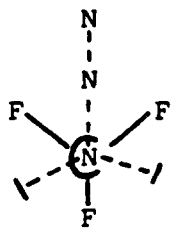

(IV)

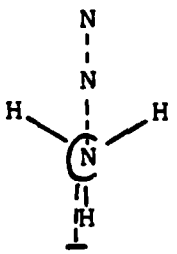

(V)

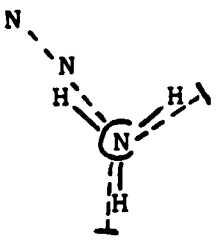

(VI)

a significant contribution from resonance structure (III). For this structure configuration (IV) minimizes the repulsion between the fluorine free valence electrons and the two sterically active free electron pairs on the N_α atom (indicated by broken lines in (IV). In contrast to CF_3N_3, the CH_3 group in CH_3N_3 appears to be in an intermediate position between eclipsed and staggered[7b], (25±7° from the eclipsed position) which may be explained in the following manner: resonance structure (II) should result in a staggered (V) and resonance structure (III) in an eclipsed (VI) configuration. Since, as discussed above, the bond lengths indicate that structure (II) contributes more strongly to the structure of CH_3N_3 than to that of CF_3N_3, the observation of an

intermediate torsional angle is not surprising.

Linearity of the N_3 Group and CF_3 Tilt Angle. In CF_3N_3 the N_3 group is slightly (10°) bent away from the CF_3 group, and the CF_3 group is tilted away from the N_3 group by 5.8°. This is readily explained by the repulsion between the fluorine free valence electron pairs and the π bond electron system of the N_3 group. A comparison of these values with those in CH_3N_3 would be most interesting, but unfortunately no experimental values are presently available for CH_3N_3. It is interesting to note that the angles of the N_3 group found for HN_3, ClN_3, NCN_3, and CF_3N_3 are all very similar. However, it should be kept in mind that most of these values carry rather large uncertainties.

Torsional Effects on the Structure. The present data for the excited torsional states do not allow a determination of the structural changes upon excitation of ν_{15}. It is clear from model calculations, however, that several parameters must change their value in order to reproduce the rotational constants of the excited states. Thus heavy relaxation, not only in the trifluoro methyl group, but also in the tilt and the $CN_\alpha N_\beta$ angle, is assumed to take place.

ACKNOWLEDGEMENT

We are grateful to Dr. G. Pawelke for providing a sample of CF_3N_3 for the RFMWDR measurements. D. Christen and H. Oberhammer acknowledge financial support by the Fonds der Chemie. K. O. Christe and C. J. Schack thank the Office of Naval Research and the U.S. Army Research Office for financial support.

References

(1) (a) Rocketdyne (b) University of Tübingen

(2) "The Chemistry of the Azido Group"; Patai, S., Ed.; Wiley-Interscience: New York, 1971.

(3) Dehnicke, K. Adv. Inorg. Chem. Radiochem. 1983, 26,169.

(4) Makarov, S. P.; Yakubovich, A. Ya.; Ginsburg, V. A.; Filatov, A. S.; Englin, M. A.; Privezentseva, N. F.; Nikiforova, T. Ya. Dokl. Akad. Nauk SSSR 1961, 141,357.

(5) Makarov, S. P.; Yakubovich, A. Ya.; Filatov, A. S.; Englin, M. A.; Nikiforova, T. Ya. Zh. Obshch. Khim. 1968, 38,709.

(6) Christe, K. O.; Schack, C. J. Inorg. Chem. 1981, 20,2566.

(7) (a) Livingston, R. L.; Rao, C. N. R. J. Phys. Chem. 1960, 64,756. (b) Anderson, D. W. W.; Rankin, D. W. H.; Robertson, A. J. Mol. Struct. 1972, 14,385.

(8) Salathiel, W. M.; Curl, R. F. Jr. J. Chem. Phys. 1966, 44,1288.

(9) Oberhammer, H. J. Fluorine Chem. 1983, 23,147.

(10) Supplementary data available (see masthead page).

(11) Haase, J. Z. Natuforsch. 1970, A25,936.

(12) Oberhammer, H. J. Chem. Phys. 1978, 69,468.

(13) Typke, V.; Dakkhouri, M.; Oberhammer, H. J. Mol. Struct. 1978, 44,85.

(14) Christen, D. J. Mol. Struct. 1978, 48,101.

(15) Muenter, J. S. J. Chem. Phys. 1968, 48,4544.

(16) Nesbitt, Jr., A. S.; Wilson, Jr., E. B. Rev. Sci. Instr. 1963, 34,901.

(17) Wodarczyk, F. J.; Wilson, Jr., E. B. J. Mol. Spectr. 1971, 37,445.

(18) Winnewisser, B. P. J. Mol. Spectr. 1980, 82,220.

(19) Dakkhouri, M.; Oberhammer, H. Z. Naturforsch. 1972, 27A,1331.

(20) Cook, R. L.; Gerry, M. C. L. J. Chem. Phys. 1970, 53,2525.

(21) Almenningen, A.; Bak, B.; Jansen, P.; Strand, T. G. Acta Chim. Scand. 1973, 27,1531.

(22) Tokue, J.; Fukuyama, T.; Kuchitsu, K. J. Mol. Struct. 1973, 17,207.

(23) Almenningen, A.; Anfinsen, I. M.; Haaland, A. Acta Chim. Scand. 1970, 24,43.

(24) Bürger, H.; Pawelke, G.; Oberhammer, H. J. Mol. Struct. 1982, 84,49.

(25) Chiang, C. H.; Porter, R. F.; Bauer, S. H. J. Am. Chem. Soc. 1970, 92,5315.

(26) Almenningen, A.; Anfinsen, I. M.; Haaland, A. Acta Chim. Scand. 1970, 24,1230.

Table 1. Interatomic distances, vibrational amplitudes from spectroscopic and electron diffraction data (error limits are 3σ values) and vibrational corrections Δ (in Å).

atom pair	r_{ij}	vibrational amplitudes spectr.	e.d.	$\Delta=r_a-r_z$
N_β - N_ω	1.12	0.034	0.034[a]	0.0060
N_α - N_β	1.25	0.042	0.042 (4)[b]	0.0004
C - F	1.33	0.045	0.045 (4)[b]	0.0013
C - N_α	1.43	0.053	0.053 (4)[b]	-0.0001
F..F	2.16	0.054	0.056 (3)[c]	0.0009
N_α..F_t	2.18	0.061	0.063 (3)[c]	0.0004
N_α..F_g	2.30	0.063		0.0001
C..N_β	2.23	0.067	0.067[a]	-0.0006
N_α..N_ω	2.36	0.046	0.046[a]	0.0028
N_β..F_g	2.71	0.169	0.174 (26)	-0.0072
C..N_ω	3.27	0.085	0.095 (40)	-0.0003
N_β..F_t	3.31	0.092	0.092[a]	0.0021
N_ω..F_g	3.56	0.229	0.250 (33)	-0.0096
N_ω..F_t	4.42	0.141	0.096 (57)	0.0130

[a]Not refined, [b,c]Ratio constrained to spectroscopic ratio.

Table 2. Geometric parameters (Å and degrees) for CF_3N_3 from electron diffraction and combined electron diffraction - microwave analysis.

	e.d.[a] r_α^o	e.d. + m.w.[b] r_{av}
C-F	1.329 (3)	1.328 (2)
$C-N_\alpha$	1.427 (5)	1.425 (5)
$N_\alpha-N_\beta$	1.250 (7)	1.252 (5)
$N_\beta-N_\omega$	1.117 (4)	1.118 (3)
$CN_\alpha N_\beta$	111.8 (1.1)	112.4 (0.2)
$N_\alpha N_\beta N_\omega$[c]	175.3 (4.3)	169.6 (3.4)
FCF	108.4 (0.4)	108.7 (0.2)
tilt[d]	4.4 (1.2)	5.8 (0.4)

[a]Results from electron diffraction analysis; error limits are 2σ values and include a possible scale error of 0.1% for bond lengths.

[b]Results from combined electron diffraction - microwave analysis; error limits are 2σ values.

[c]Bend away from CF_3 group.

[d]Tilt of CF_3 group away from N_3 group.

Table 3. Force Field[a] for CF_3N_3

CF	6.69	CF/CF	1.06
CN	4.84	CF/CN	0.46
$N_\alpha N_\beta$	7.75	CF/FCF (adj)	0.51
$N_\beta N_\omega$	16.88	CF/FCF (opp)	-0.33
FCF	1.82	CN/FCF	-1.00
NCF	1.20	CN/NCF (adj)	0.42
CNN	1.49	CN/NNN	-0.54
NNN	0.67	FCF/FCF	0.23
tors	0.03	FCF/NNN	-0.18
		NNN/tors	-0.07

[a]Stretch in mdyn/Å, stretch/bend in mdyn/rad, bend in mdynÅ/rad^2

Table 4. Measured rotational transitions and derived rotational constants (MHz).

	v = 0	v_{15} = 1	v_{15} = 2	v_{15} = 3	v_{15} = 4[a]	v_{10} = 1	v_{10} = 2	v_{15} = 1, v_{10} = 1 v_9 = 1	
$1_{01}2_{02}$	7845.90	7848.36	7851.39	7854.87	7858.13	7851.84	7857.67	7853.68	
$2_{12}3_{13}$	11738.22	11750.70	11764.13	11778.62		11743.79	11749.23	11755.80	
$2_{02}3_{03}$	11768.73	11772.52	11777.05	11782.32	11787.38	11777.53		11780.40	
$2_{21}3_{22}$	11768.73	11772.33	11776.69	11781.82		11777.72		11780.28	
$2_{20}3_{21}$	11768.93	11772.49	11776.69	11781.82		11778.00		11780.51	
$2_{11}3_{12}$	11799.67	11794.40	11789.80	11785.77				11805.19	
$4_{14}5_{15}$	19563.32	19584.34	19606.66	19630.92		19572.60	19581.52	19592.76	
$4_{41}5_{42}$ $4_{40}5_{41}$	19612.98	19618.70	19625.77	19633.66		19627.90		19632.07	
$4_{04}5_{05}$	19613.36	19620.17	19627.90	19637.11	19646.89	19627.75	19641.95	19633.17	
$4_{32}5_{33}$ $4_{31}5_{32}$	19614.09	19619.84	19626.93	19635.37		19629.06	19643.67	19633.17	
$4_{23}5_{24}$	19614.28	19620.17	19627.75	19636.38		19629.06	19643.67	19633.58	
$4_{22}5_{23}$	19615.96	19621.02	19627.90	19636.38			19646.29	19634.74	
$4_{13}5_{14}$	19665.79	19657.02	19649.58	19642.92		19686.00	19706.00	19675.23	
$5_{15}6_{16}$	23475.69	23500.96	23527.92	23557.02		23486.68	23497.42	23510.98	23480.85
$5_{51}6_{52}$ $5_{50}6_{51}$	23534.01	23540.81	23549.30			23551.87			
$5_{05}6_{06}$	23534.97	23543.71	23553.54	23564.72		23552.18	23568.80		
$5_{42}6_{43}$ $5_{41}6_{42}$	23535.65	23542.48	23551.08	23560.39		23553.51			
$5_{24}6_{25}$	23536.98	23544.36	23553.06	23563.73		23554.88		23560.39	
$5_{33}6_{34}$ $5_{32}6_{33}$	23537.01	23543.71	23552.40	23562.22		23554.88			
$5_{23}6_{24}$	23540.01	23545.76	23553.54	23563.73		23558.48		23562.22	
$5_{14}6_{15}$	23598.62	23588.29	23579.39	23571.50		23662.84	23646.77	23609.94	23607.58
A[b]	5544.	5631.5	5722.4	5817.2	5880.5	5517.5	5490.	5600.	5526.5
B	1971.750(4)	1969.374(6)	1967.121(6)	1964.924(7)	3929.1[c]	1974.335(6)	1976.896(5)	1971.679(6)	1967.30
C	1951.260(4)	1954.825(6)	1958.544(6)	1962.519(7)		1951.648(6)	1952.002(5)	1955.188(6)	1956.74
D_{JK}[d]	0.0142(1)	0.0150(2)	0.0158(2)	0.0220(31)		0.0143(2)	0.0141(5)	0.0148(3)	0.[e]

[a] A species, [b] fixed to value determined from structural model and harmonic effects, [c] B + C, [d] kHz, [e] assumed.

Table 5. Principal geometric parameters of some azides, XN_3, studied in the gas phase.

	HN_3[b]	CH_3N_3[c]	Me_3SiN_3[d]	ClN_3[e]	NCN_3[f]	CF_3N_3[g]
$X-N_\alpha$	1.015 (15)	1.468 (5)	1.734 (7)	1.745 (5)	1.355 (2)	1.425 (5)
$N_\alpha - N_\beta$	1.243 (5)	1.216 (4)	1.198 (8)	1.252 (10)	1.261 (2)	1.252 (5)
$N_\beta - N_\omega$	1.134 (2)	1.130 (5)	1.150 (11)	1.133 (10)	1.121 (2)	1.118 (3)
$XN_\alpha N_\beta$	108.8 (4.0)	116.8 (0.3)	128.0 (1.6)	108.7 (0.5)	114.5 (0.2)	112.4 (0.2)
$N_\alpha N_\beta N_\omega$	171.3 (5.0)	180[h]	180[h]	171.9 (0.5)	169.2 (1.6)	169.6 (3.4)
τ[a]	---	35.0 (7.0)	24.0 (5.0)	---	---	0.0

[a] Torsional angle of group X around X-N bond. $\tau = 0$ corresponds to staggered position.

[b] r_s values, Ref. 18. [c] r_a values, Ref. 7b. [d] r_a values, Ref. 19. [e] r_s/r_o values, Ref. 20.

[f] r_α values, Ref. 21. [g] r_{av} values, this study. [h] estimated value.

Figure Captions

1. Experimental (.....) and calculated (———) molecular intensities and differences.

2. Experimental radial distribution function, theoretical functions for staggered and eclipsed conformations and difference curve between experimental and theoretical staggered conformation.

3. The J: 4→5 rotational transitions. Stark field: 200 V/cm. Arrows indicate frequencies at which $K_{-1} = 0$ lines appear at higher Stark fields.

   $v_T = v_{15}$. $v_T = 4$ indicates the center of the A components of the torsionally split $v_T = 4$ state. The $K_{-1} = 1$ lines have not definitively been assigned.

4. The J: $5_{15} \rightarrow 6_{16}$ transitions showing several vibrationally excited states at a Stark field of 800 V/cm. $v_T = v_{15}$.

5. The J: $1_{01} \rightarrow 2_{02}$ transitions at a Stark field of 800 V/cm. Marker spacing is 0.8 MHz. The assignment of $v_T = 4$ is speculative, although other J candidates for the A components have been located.

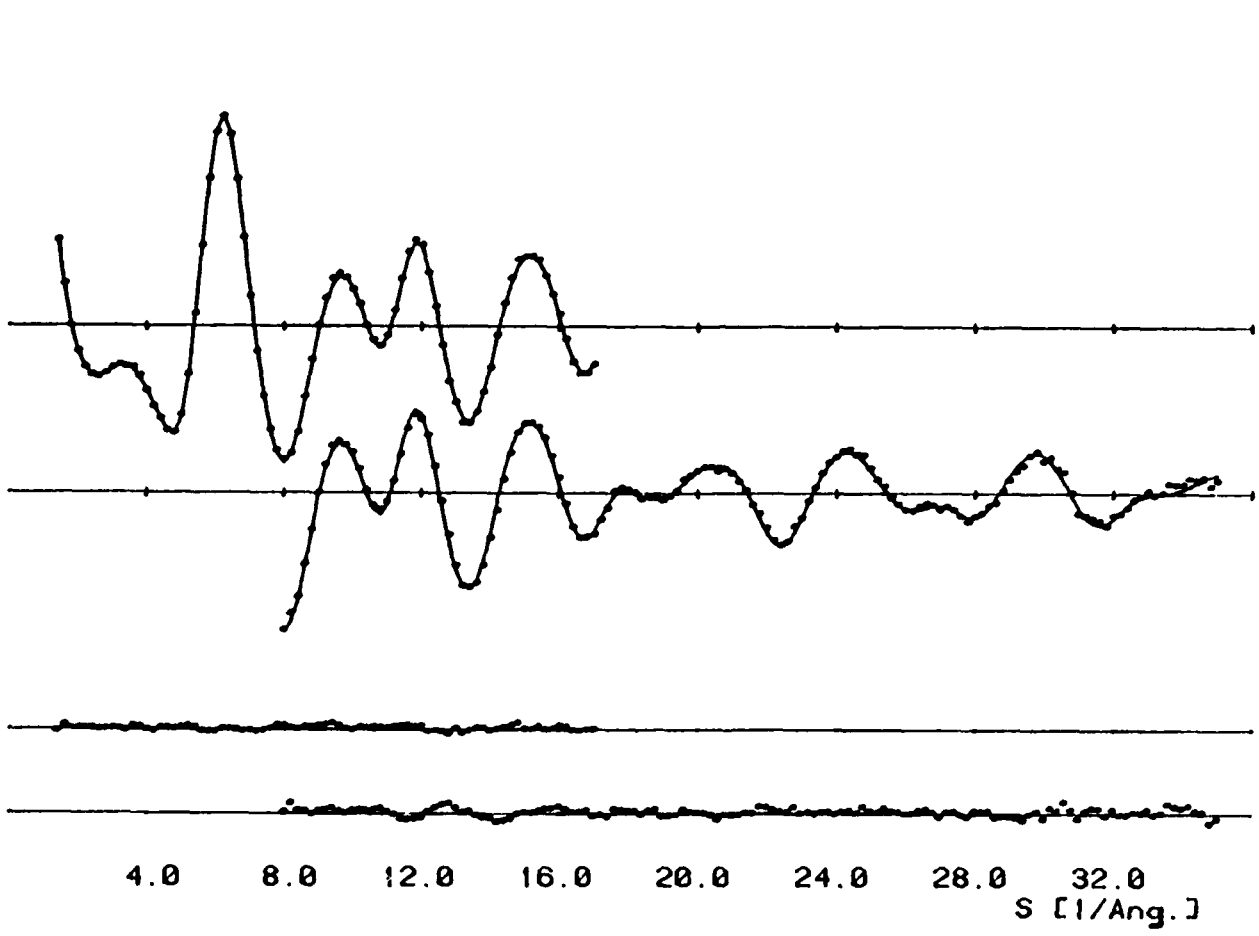

FIGURE 1.

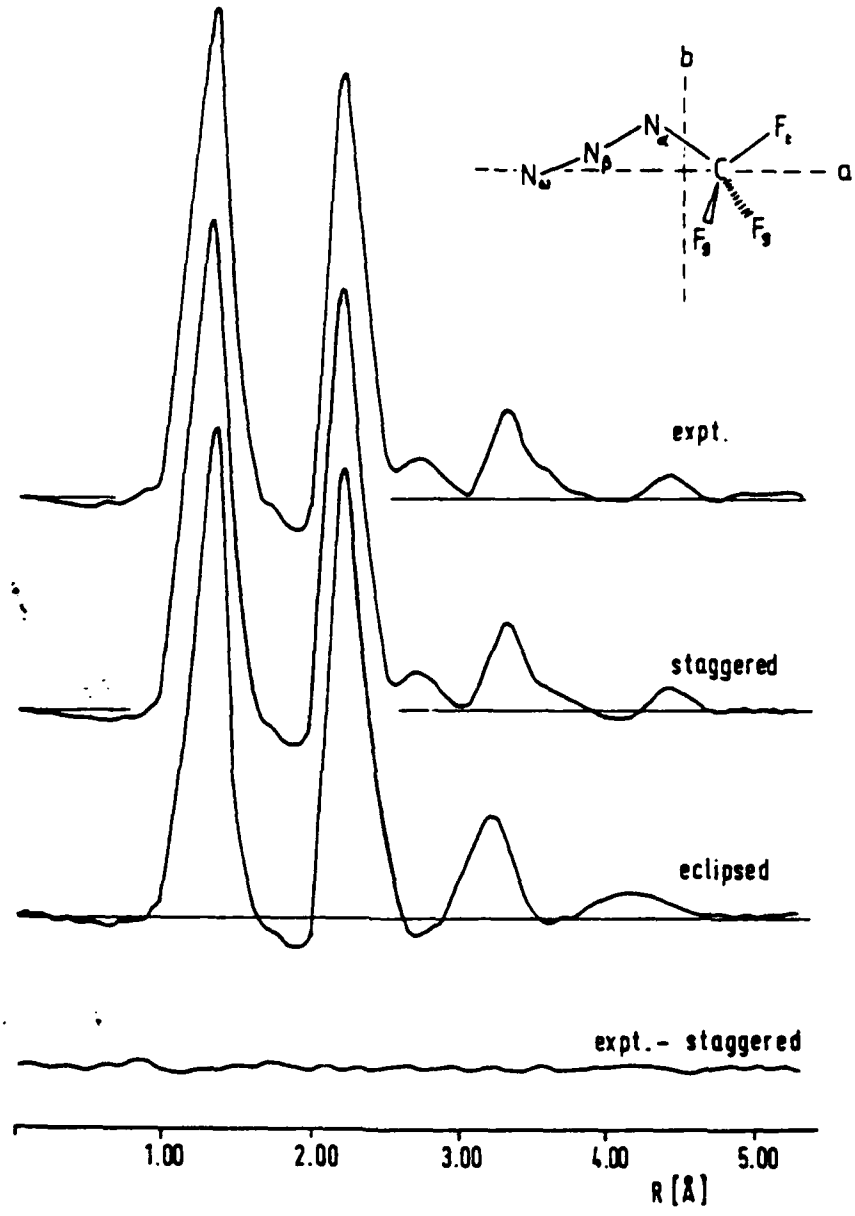
b
a
N_γ
N_β
N_α
C
F_t
F_g
F_g
expt.
staggered
eclipsed
expt.- staggered
1.00
2.00
3.00
4.00
5.00
R [Å]

FIGURE 2.

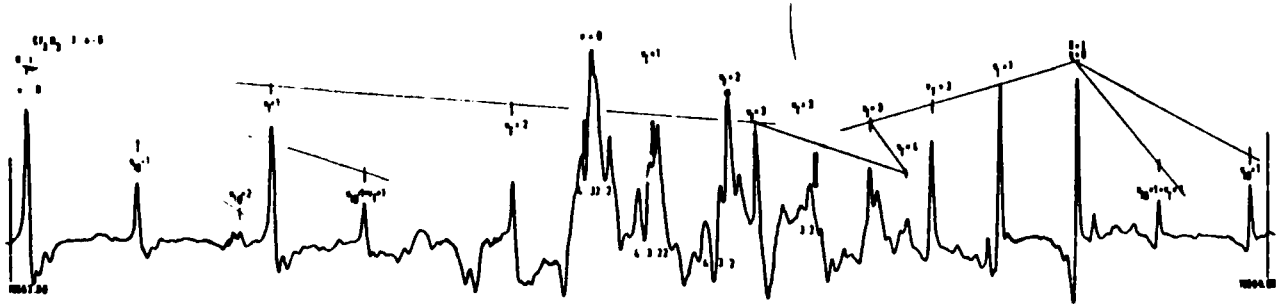

FIGURE 3.

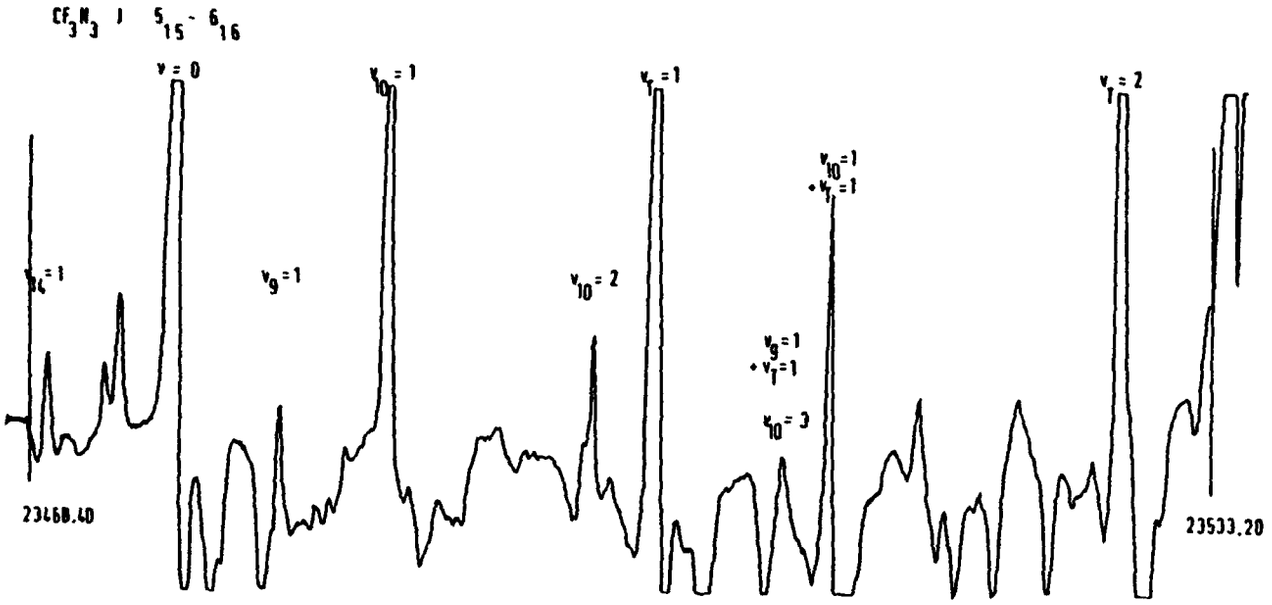
CF_3N_3 J $5_{15} - 6_{16}$
v = 0
ν_{10} = 1
ν_7 = 1
ν_7 = 2
ν_{10} = 1
+ ν_7 = 1
ν_4 = 1
ν_9 = 1
ν_{10} = 2
ν_9 = 1
+ ν_7 = 1
ν_{10} = 3
23468.40
23533.20

FIGURE 4.

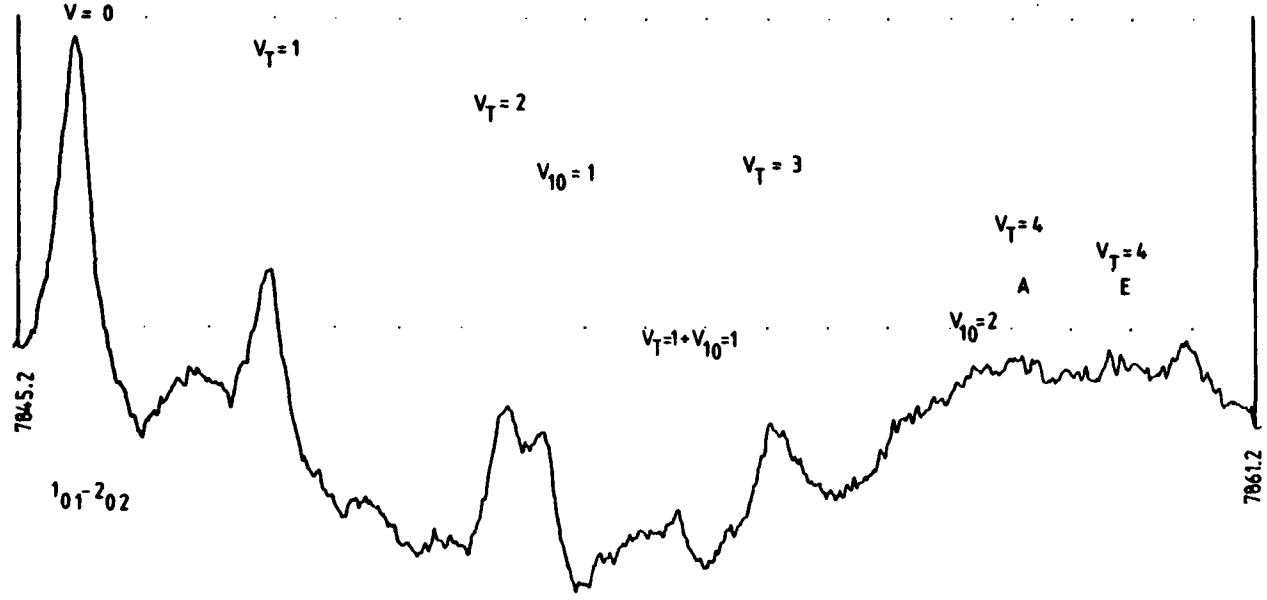
V = 0
$V_T = 1$
$V_T = 2$
$V_{10} = 1$
$V_T = 3$
$V_T = 4$
A
$V_T = 4$
E
$V_{10} = 2$
$V_T = 1 + V_{10} = 1$
7845.2
$^1O_1 - ^2O_2$
7861.2

FIGURE 5.

Supplementary Data

Total electron diffraction intensities for two camera distances (50 and 25 cm) for two sets of plates (2 pages).

TOTAL INTENSITIES FOR CF3N3 50 CM CAMERA DISTANCE PLATE NO 3

1.4	0.2276	5.4	0.2356	9.4	0.2011	13.4	0.1462
1.6	0.2108	5.6	0.2585	9.6	0.1992	13.6	0.1462
1.8	0.1944	5.8	0.2798	9.8	0.1957	13.8	0.1473
2.0	0.1811	6.0	0.2914	10.0	0.1916	14.0	0.1484
2.2	0.1715	6.2	0.2919	10.2	0.1872	14.2	0.1500
2.4	0.1678	6.4	0.2827	10.4	0.1812	14.4	0.1521
2.6	0.1685	6.6	0.2663	10.6	0.1775	14.6	0.1536
2.8	0.1750	6.8	0.2471	10.8	0.1746	14.8	0.1541
3.0	0.1846	7.0	0.2294	11.0	0.1742	15.0	0.1533
3.2	0.1928	7.2	0.2128	11.2	0.1756	15.2	0.1520
3.4	0.1968	7.4	0.1995	11.4	0.1774	15.4	0.1508
3.6	0.2018	7.6	0.1902	11.6	0.1784	15.6	0.1485
3.8	0.2012	7.8	0.1841	11.8	0.1777	15.8	0.1467
4.0	0.1974	8.0	0.1804	12.0	0.1754	16.0	0.1446
4.2	0.1927	8.2	0.1804	12.2	0.1702	16.2	0.1424
4.4	0.1902	8.4	0.1829	12.4	0.1646	16.4	0.1400
4.6	0.1877	8.6	0.1883	12.6	0.1591	16.6	0.1388
4.8	0.1887	8.8	0.1933	12.8	0.1533	16.8	0.1389
5.0	0.1970	9.0	0.1976	13.0	0.1499	17.0	0.1388
5.2	0.2136	9.2	0.2002	13.2	0.1471		

TOTAL INTENSITIES FOR CF3N3 25 CM CAMERA DISTANCE PLATE NO 8

8.0	0.1824	14.8	0.1976	21.6	0.1792	28.4	0.1785
8.2	0.1856	15.0	0.1978	21.8	0.1785	28.6	0.1786
8.4	0.1882	15.2	0.1974	22.0	0.1774	28.8	0.1789
8.6	0.1934	15.4	0.1966	22.2	0.1769	29.0	0.1793
8.8	0.1988	15.6	0.1954	22.4	0.1766	29.2	0.1797
9.0	0.2040	15.8	0.1936	22.6	0.1767	29.4	0.1797
9.2	0.2081	16.0	0.1914	22.8	0.1770	29.6	0.1799
9.4	0.2105	16.2	0.1892	23.0	0.1775	29.8	0.1800
9.6	0.2106	16.4	0.1871	23.2	0.1784	30.0	0.1796
9.8	0.2096	16.6	0.1858	23.4	0.1789	30.2	0.1796
10.0	0.2082	16.8	0.1852	23.6	0.1793	30.4	0.1788
10.2	0.2054	17.0	0.1855	23.8	0.1799	30.6	0.1783
10.4	0.2023	17.2	0.1859	24.0	0.1800	30.8	0.1776
10.6	0.2003	17.4	0.1863	24.2	0.1805	31.0	0.1770
10.8	0.1995	17.6	0.1868	24.4	0.1807	31.2	0.1765
11.0	0.2001	17.8	0.1865	24.6	0.1805	31.4	0.1763
11.2	0.2020	18.0	0.1859	24.8	0.1804	31.6	0.1758
11.4	0.2044	18.2	0.1853	25.0	0.1798	31.8	0.1750
11.6	0.2066	18.4	0.1845	25.2	0.1793	32.0	0.1747
11.8	0.2076	18.6	0.1841	25.4	0.1789	32.2	0.1753
12.0	0.2066	18.8	0.1839	25.6	0.1784	32.4	0.1754
12.2	0.2041	19.0	0.1837	25.8	0.1782	32.6	0.1756
12.4	0.2003	19.2	0.1834	26.0	0.1781	32.8	0.1754
12.6	0.1967	19.4	0.1832	26.2	0.1782	33.0	0.1752
12.8	0.1931	19.6	0.1835	26.4	0.1782	33.2	0.1746
13.0	0.1898	19.8	0.1833	26.6	0.1784	33.4	0.1744
13.2	0.1877	20.0	0.1831	26.8	0.1784	33.6	0.1742
13.4	0.1870	20.2	0.1829	27.0	0.1785	33.8	0.1740
13.6	0.1870	20.4	0.1826	27.2	0.1786	34.0	0.1734
13.8	0.1883	20.6	0.1824	27.4	0.1784	34.2	0.1729
14.0	0.1904	20.8	0.1821	27.6	0.1783	34.4	0.1728
14.2	0.1926	21.0	0.1813	27.8	0.1782	34.6	0.1730
14.4	0.1948	21.2	0.1808	28.0	0.1781	34.8	0.1733
14.6	0.1964	21.4	0.1803	28.2	0.1783	35.0	0.1736

TOTAL INTENSITIES FOR CF3N3 50 CM CAMERA DISTANCE PLATE NN 5

1.4	0.3680	5.4	0.4317	9.4	0.3770	13.4	0.2856
1.6	0.3546	5.6	0.4682	9.6	0.3750	13.6	0.2905
1.8	0.3360	5.8	0.4987	9.8	0.3699	13.8	0.2917
2.0	0.3204	6.0	0.5183	10.0	0.3631	14.0	0.2950
2.2	0.3124	6.2	0.5229	10.2	0.3544	14.2	0.2987
2.4	0.3122	6.4	0.5080	10.4	0.3465	14.4	0.3024
2.6	0.3178	6.6	0.4816	10.6	0.3389	14.6	0.3047
2.8	0.3306	6.8	0.4509	10.8	0.3348	14.8	0.3063
3.0	0.3476	7.0	0.4213	11.0	0.3342	15.0	0.3054
3.2	0.3602	7.2	0.3946	11.2	0.3364	15.2	0.3042
3.4	0.3686	7.4	0.3746	11.4	0.3404	15.4	0.3023
3.6	0.3763	7.6	0.3583	11.6	0.3426	15.6	0.2991
3.8	0.3768	7.8	0.3480	11.8	0.3412	15.8	0.2959
4.0	0.3708	8.0	0.3428	12.0	0.3374	16.0	0.2918
4.2	0.3641	8.2	0.3426	12.2	0.3292	16.2	0.2880
4.4	0.3587	8.4	0.3482	12.4	0.3199	16.4	0.2849
4.6	0.3538	8.6	0.3562	12.6	0.3100	16.6	0.2826
4.8	0.3552	8.8	0.3646	12.8	0.3021	16.8	0.2819
5.0	0.3702	9.0	0.3718	13.0	0.2970	17.0	0.2827
5.2	0.3963	9.2	0.3759	13.2	0.2913		

TOTAL INTENSITIES FOR CF3N3 25 CM CAMERA DISTANCE PLATE NN 10

8.0	0.1974	14.6	0.2078	21.6	0.1900	28.4	0.1901
8.2	0.2003	15.0	0.2082	21.8	0.1893	28.6	0.1901
8.4	0.2031	15.2	0.2076	22.0	0.1886	28.8	0.1904
8.6	0.2060	15.4	0.2072	22.2	0.1873	29.0	0.1909
8.8	0.2133	15.6	0.2057	22.4	0.1872	29.2	0.1912
9.0	0.2178	15.8	0.2042	22.6	0.1876	29.4	0.1913
9.2	0.2214	16.0	0.2021	22.8	0.1880	29.6	0.1914
9.4	0.2234	16.2	0.1998	23.0	0.1884	29.8	0.1916
9.6	0.2235	16.4	0.1978	23.2	0.1892	30.0	0.1912
9.8	0.2222	16.6	0.1964	23.4	0.1901	30.2	0.1915
10.0	0.2206	16.8	0.1961	23.6	0.1906	30.4	0.1911
10.2	0.2178	17.0	0.1953	23.8	0.1911	30.6	0.1905
10.4	0.2147	17.2	0.1959	24.0	0.1914	30.8	0.1897
10.6	0.2122	17.4	0.1963	24.2	0.1915	31.0	0.1881
10.8	0.2109	17.6	0.1970	24.4	0.1919	31.2	0.1882
11.0	0.2113	17.8	0.1970	24.6	0.1919	31.4	0.1882
11.2	0.2131	18.0	0.1961	24.8	0.1919	31.6	0.1878
11.4	0.2158	18.2	0.1955	25.0	0.1914	31.8	0.1840
11.6	0.2180	18.4	0.1947	25.2	0.1907	32.0	0.1875
11.8	0.2190	18.6	0.1946	25.4	0.1906	32.2	0.1870
12.0	0.2178	18.8	0.1942	25.6	0.1900	32.4	0.1875
12.2	0.2156	19.0	0.1938	25.8	0.1899	32.6	0.1879
12.4	0.2120	19.2	0.1938	26.0	0.1896	32.8	0.1872
12.6	0.2076	19.4	0.1938	26.2	0.1894	33.0	0.1870
12.8	0.2034	19.6	0.1941	26.4	0.1898	33.2	0.1864
13.0	0.2000	19.8	0.1940	26.6	0.1899	33.4	0.1864
13.2	0.1978	20.0	0.1939	26.8	0.1897	33.6	0.1865
13.4	0.1968	20.2	0.1936	27.0	0.1901	33.8	0.1861
13.6	0.1971	20.4	0.1932	27.2	0.1902	34.0	0.1860
13.8	0.1984	20.6	0.1928	27.4	0.1902	34.2	0.1859
14.0	0.2004	20.8	0.1926	27.6	0.1898	34.4	0.1860
14.2	0.2023	21.0	0.1921	27.8	0.1894	34.6	0.1858
14.4	0.2046	21.2	0.1917	28.0	0.1896	34.8	0.1860
14.6	0.2063	21.4	0.1907	28.2	0.1897	35.0	0.1864

DL/413/83/01
GEN/413-2

TECHNICAL REPORT DISTRIBUTION LIST, GEN

	No. Copies
Office of Naval Research Attn: Code 413 800 N. Quincy Street Arlington, Virginia 22217	2
ONR Pasadena Detachment Attn: Dr. R. J. Marcus 1030 East Green Street Pasadena, California 91106	1
Commander, Naval Air Systems Command Attn: Code 310C (H. Rosenwasser) Washington, D.C. 20360	1
Naval Civil Engineering Laboratory Attn: Dr. R. W. Drisko Port Hueneme, California 93401	1
Superintendent Chemistry Division, Code 6100 Naval Research Laboratory Washington, D.C. 20375	1
Defense Technical Information Center Building 5, Cameron Station Alexandria, Virginia 22314	12
DTNSRDC Attn: Dr. G. Bosmajian Applied Chemistry Division Annapolis, Maryland 21401	1
Naval Ocean Systems Center Attn: Dr. S. Yamamoto Marine Sciences Division San Diego, California 91232	1
Naval Ocean Systems Center Attn: Technical Library San Diego, California 92152	1
Naval Weapons Center Attn: Dr. A. B. Amster Chemistry Division China Lake, California 93555	1
Scientific Advisor Commandant of the Marine Corps Code RD-1 Washington, D.C. 20380	1
Dean William Tolles Naval Postgraduate School Monterey, California 93940	1
U.S. Army Research Office Attn: CRD-AA-IP P.O. Box 12211 Research Triangle Park, NC 27709	1
Mr. Vincent Schaper DTNSRDC Code 2830 Annapolis, Maryland 21402	1
Mr. John Boyle Materials Branch Naval Ship Engineering Center Philadelphia, Pennsylvania 19112	1
Mr. A. M. Anzalone Administrative Librarian PLASTEC/ARRADCOM Bldg 3401 Dover, New Jersey 07801	1

TECHNICAL REPORT DISTRIBUTION LIST, 053

Dr. M. F. Hawthorne
Department of Chemistry
University of California
Los Angeles, California 90024

Dr. D. Venezky
Chemistry Division
Naval Research Laboratory
Washington, D.C. 20375

Professor O. T. Beachley
Department of Chemistry
State University of New York
Buffalo, New York 14214

Dr. A. Cowley
Department of Chemistry
University of Texas
Austin, Texas 78712

Dr. W. Hatfield
Department of Chemistry
University of North Carolina
Chapel Hill, North Carolina 27514

Professor Richard Eisenberg
Department of Chemistry
University of Rochester
Rochester, New York 14627

Professor K. Niedenzu
Department of Chemistry
University of Kentucky
Lexington, Kentucky 40506

Dr. T. Marks
Department of Chemistry
Northwestern University
Evanston, Illinois 60201

Dr. J. Zuckerman
Department of Chemistry
University of Oklahoma
Norman, Oklahoma 73019

Professor K. M. Nicholas
Department of Chemistry
Boston College
Chestnut Hill, Massachusetts 02167

Professor R. Neilson
Department of Chemistry
Texas Christian University
Fort Worth, Texas 76129

Professor M. Newcomb
Department of Chemistry
Texas A&M University
College Station, Texas 77843

Professor R. Wells
Department of Chemistry
Duke University
Durham, North Carolina 27706

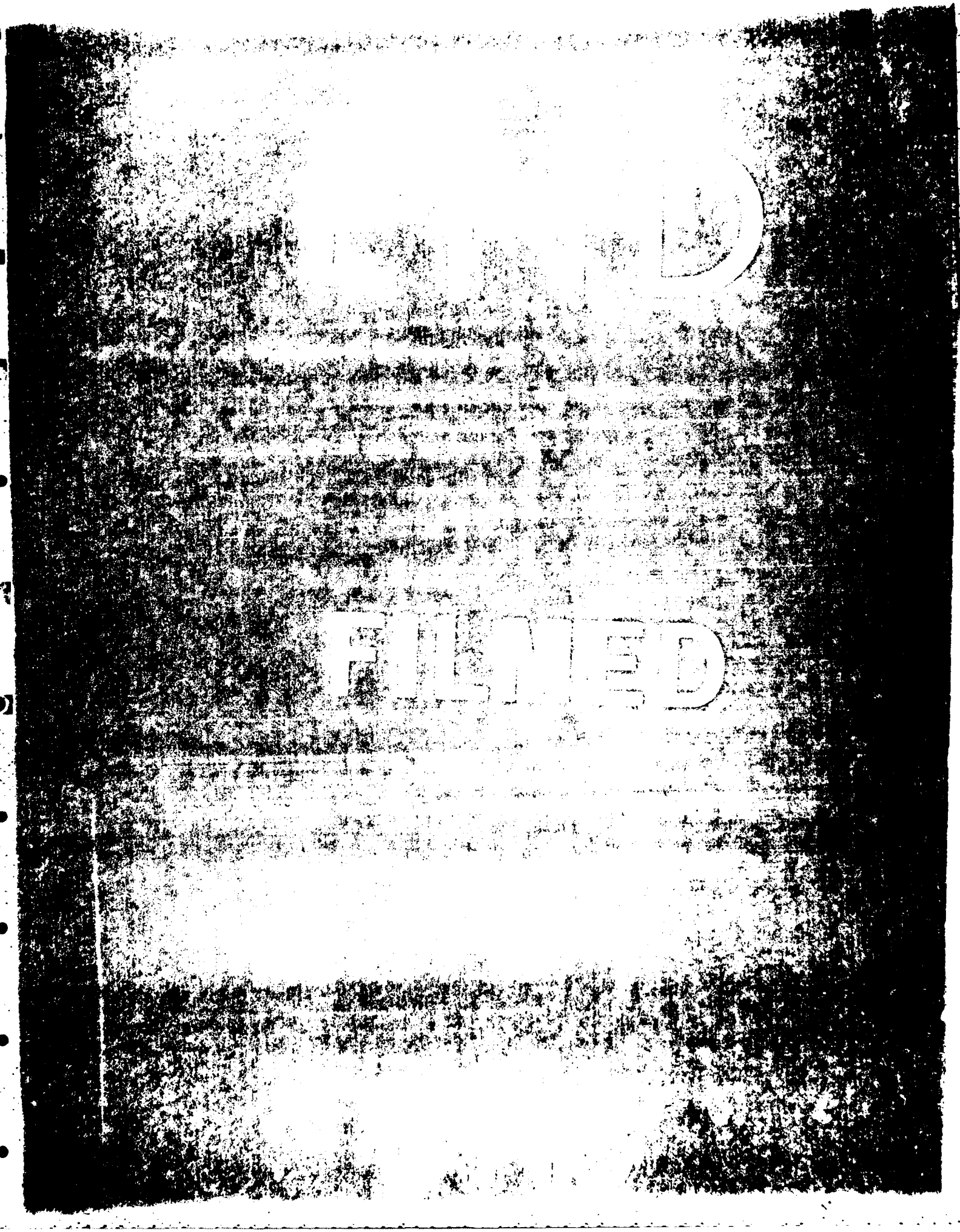
FILMED